



Cross-validated Adaboost Classification of Emotion Regulation Strategies Identified by Spectral Coherence in Resting-State

Serap Aydin¹

Accepted: 18 August 2021 / Published online: 18 September 2021

© The Author(s), under exclusive licence to Springer Science+Business Media, LLC, part of Springer Nature 2021

Abstract

In the present study, quantitative relations between Cognitive Emotion Regulation strategies (CERs) and EEG synchronization levels have been investigated for the first time. For this purpose, spectral coherence (COH), phase locking value and mutual information have been applied to short segments of 62-channel resting state eyes-opened EEG data collected from healthy adults who use contrasting emotion regulation strategies (frequently and rarely use of rumination&distraction, frequently and rarely use of suppression&reappraisal). In tests, the individuals are grouped depending on their self-responses to both emotion regulation questionnaire (ERQ) and cognitive ERQ. Experimental data are downloaded from publicly available database, LEMON. Regarding EEG electrode pairs that placed on right and left cortical regions, inter-hemispheric dependency measures are computed for non-overlapped short segments of 2 sec at 2 min duration trials. In addition to full-band EEG analysis, dependency metrics are also obtained for both alpha and beta sub-bands. The contrasting groups are discriminated from each other with respect to the corresponding features using cross-validated adaboost classifiers. High classification accuracies (CA) of 99.44% and 98.33% have been obtained through instant classification driven by full-band COH estimations. Considering regional features that provide the high CA, CERs are found to be highly relevant with associative memory functions and cognition. The new findings may indicate the close relation between neuroplasticity and cognitive skills.

Keywords Emotion regulation · Brain biophysics · EEG · Coherence

Introduction

Cognitive Emotion Regulation strategies (CERs) enable us to control our emotional responses by means of both face/body expression and cognitive functions. Therefore, both daily and business life are highly oriented by cognitive skills on regulation of emotions (Ochsner & Gross, 2008). Four different strategies can be defined in CERs: Rumination (RU) is characterized by negative and depressive thoughts (Gross, 2002). Cognitive Distraction (CD) is the opposite of RU such that; The person can orient his/her attention to pleasant thoughts to avoid the depressed mood and tends to move away from the negative matter (Phan et al., 2005; Webb et al., 2012). Expressive Suppression (ES) is intended to regulate the outward, or behavioral, emotional response, however, it is paradoxical in regulating internal emotional

response. In detail, ES suppresses negative emotions, such as sadness or anxiety, with positive behavioral body/face expressions. Thus, using SE increases the felt intensity of negative emotions. During positive emotions, such as happiness, using ES reduces the experience of positive emotions (Gross & Jazaieri, 2014). Cognitive Reappraisal (CR) reflects an effort to change the subjective evaluation of an emotion-generating situation to modify its emotional impact (Gross & Jazaieri, 2014). Both self- and peer-reports show that controlling emotions with CR yields affective benefits in comparison to ES. Using CR is associated with more internally felt and outwardly expressed positive emotion as well as less internally felt and outwardly expressed negative emotion (Kalokerinos et al., 2014).

Mainly, neuro-cognitive studies have focused on the neuroimaging analysis in individuals who frequently use one of these CERs so far. In particular, structural and functional brain differences have been shown in between two contrasting CERs, i.e. RU vs CD in response to emotional stimuli (Goldin et al., 2008). Regarding gray matter volume and surface thickness in resting state functional MRI studies,

✉ Serap Aydin
serap.aydin@hacettepe.edu.tr

¹ Biophysics Department, Medical Faculty, Hacettepe University, Ankara, Turkey

structural variations have been found to be associated with both ES (Giuliani et al., 2011a; Wang et al., 2017) and CR in mostly prefrontal cortex (Giuliani et al., 2011b). As well, task-based functional MRI studies reveal the close correlation of brain structure with both ES (Goldin et al., 2008; Lee et al., 2008) and CR (Diekhof et al., 2011; Buhle et al., 2014) in prefrontal cortex, insula and amygdala.

In the present study, as a new perspective, it is aimed to understand the inter-hemispheric functional dependency managed by cognitive functions in adults who tend to use two opposite ER strategies, one of which decreases emotional intensity and the other increases emotional intensity. Inter-hemispheric functional connectivity levels have been estimated from eyes-opened EEG measurements that provide prompt and objective information about the neuro-cortical activations. However, it is crucial to use domain-specific variety of the approaches in estimating characteristic indicators of brain network. Thus, spectral coherence (COH), phase locking value (PLV), mutual information (MI) and wavelet coherence (WCOH) have been compared to each other to find the association between cognitive abilities and electro-chemical activities underlying use of opposite CERs simultaneously. For this purpose, raw EEG data collected from healthy adults, demographic info as well as psychological test scales of the participants were obtained from publicly available data-set, LEMON described in reference (Babayan et al., 2019).

Among inter-hemispheric EEG dependency approaches, COH can be considered as computationally fast and relatively robust method over relevant coherent frequencies in EEG measurements in neuroscience. Therefore, COH has been frequently used to detect and quantify coupling between brain oscillations generated by neuronal populations at two different cortical regions (Ray & Maunsell, 2010; Saalman et al., 2012; Bosman et al., 2012; Roberts et al., 2013). Since, COH value means linear phase-consistency of cross-spectral densities originated from neuro-electrical functions over a limited time windows. Besides, examining COH requires an assumption on EEG stationarity. Thus, short duration EEG segments of 2 sec were analyzed in the present study in order to overcome the possible drawbacks of stationary assumption.

PLV has been implemented to estimate quantitative phase-locking between brain oscillations based on the instantaneous phase independently stationarity assumption. Its main challenge is to decompose complex multi-components through Hilbert Transform (Le Van et al., 2001). However, PLV has been found to be useful in analysis of EEG recordings computed by averaging over multiple trials in response to external stimuli or cognitive task (Aydore et al., 2013). Different from both COH and PLV, MI quantifies the information gained about one system from the measurement of another through detecting linear and nonlinear statistical

dependencies between these two systems. Thus, MI has been used in diverse fields as a measure of coupling or information transmission between two systems. MI is notably introduced to describe neuronal transmission of post-synaptic potentials across different cortical regions in detecting sleep states (Ramanand et al., 2001) and sleep disorders (Aydin et al., 2015). As well, MI has been used to obtain electrophysiological indicators of Alzheimer Jeonga et al. (2001) and schizophrenia Na et al. (2002) in diagnose. WCOH is relatively a new dependency metric that is proposed to quantify neural coupling of cortical regions (Lachaux et al., 2002). In particular, research studies use WCOH in analysis of functional Near Infra-Red Spectroscopy (f-NIRs) measurements based on an assumption that specific cross-brain systems share processes through temporally synchronous activities (Zhang et al., 2015, 2020).

The motivation of the present study is to show the close association of resting-state healthy neuro-transmission mechanism with cognitive skills linked to mood with respect to quantitative dependency metrics with optimal arrangement of parameters and variables in examining inter-hemispheric connectivity approaches. The innovation of the present study is to use both linear and non-linear dependency methods in discriminating the healthy adults in accordance with their cognitive and behavioural emotion regulation strategies. The new findings reveal that high cortical functions emerged from frequently use of opposite ERs can be characterized by full-band (0.5 – 40.5 Hz) inter-hemispheric dependency estimations in cortical regions responsible for cognition, attention and associative motor functions. In particular, the corresponding results clearly show the specified Brodmann Areas (BAs) of 5, 6, 9, 10, 18, 37, 39, 40, 47 are responsible for cognitive skills. The corresponding contributions are to propose the useful and optimal arrangements on the configuration of filters, segmentation of resting-state EEG series, identification of the individuals and computation of power spectral density estimations in short EEG segments in obtaining quantitative indicators that refer cognitive abilities. The proposed parameters and application procedure can also be used in detecting cognitive decline and/or cognitive disorders, since resting-state functional connectivity estimations with electrophysiological measurements is an attractive research topic in studying intrinsic brain activity.

In following sections, the groups including the adults who use opposite CERs simultaneously (frequently and rarely use of both RU and CD, frequently and rarely use of both ES and CR) are introduced. A sub-section presents both instrumentation and recording principle of resting-state EEG series collected from their scalp surface. Inter-hemispheric dependency approaches (COH, PLV, MI, WCOH) are briefly defined in separate section. The use of Adaboost classification is mainly described in sub-section. The results include detailed applications of the dependency methods to both

full-band (0.5 – 40.5 Hz) and sub-band (Alpha:7.5 – 12 Hz, Beta:12.5 – 30 Hz) frequency intervals of short EEG segments in eyes-opened resting state. Overall results are discussed and concluded in accordance with Broadmann areas and recent research studies that use inter-hemispheric coherence estimations in cognitive science in the last section.

Methods

The Participants

Surface EEG measurements and the psychometric test scores of the participants were obtained from an internationally validated, accessible database, LEMON introduced in reference (Babayan et al., 2019). In collecting data, primary step was to complement cognitive test batteries lasting about 4 hours of duration each at first day. Resting-state EEG series were recorded from participants who completed both Emotion Regulation Questionnaire (EQR) and Cognitive EQR (CEQR) at second day. As well, psychiatric interview was done by experts with the participants to decide the healthy status of them. So, hypertensive patients and those with cardiological and neurological diseases are not included.

The corresponding CEQR scores shows how often the individuals use rumination and cognitive distraction strategies (Garnefski et al., 2001; Loch et al., 2011). Besides, the resulting EQR scores shows how often the individuals use cognitive reappraisal and expressive suppression strategies (Gross & John, 2003; Abler & Kessler, 2009). Therefore, the participants were firstly clustered into following groups:

- GP1** The individuals use both strategies Rumination and Distraction frequently (the quantitative rumination sub-scale is higher than $mean = 5.40$, $std = 2.62$ and the positive refocusing sub-scale is higher than $mean = 4.90$, $std = 2.58$),
- GP2** The individuals rarely use any of the strategies Rumination and Distraction (the quantitative rumination sub-scale is lower than $mean = 5.40$, $std = 2.62$ and the positive refocusing sub-scale is lower than $mean = 4.90$, $std = 2.58$),
- GP3** The individuals use both strategies Expressive Suppression and Cognitive Reappraisal frequently (the quantitative suppression sub-scale is higher than $mean = 2.92$, $std = 1.02$ and the reappraisal sub-scale is higher than $mean = 4.99$, $std = 0.89$)
- GP4** The individuals rarely use any of the strategies Expressive Suppression and Cognitive Reappraisal frequently (the quantitative suppression sub-scale is lower than $mean = 2.92$, $std = 1.02$ and the reappraisal sub-scale is lower than $mean = 4.99$, $std = 0.89$)

In defining GP1 and GP2, the sub-scales of RU and positive refocusing into 27 questions in CEQR on a 5-point Likert scale (1 refers 'almost never' to 5 refers 'almost always'), while the sub-scales of ES and CR into 10 items in EQR on a 7-point Likert scale (1 refers 'strongly disagree' to 7 refers 'strongly agree') in defining GP3 and GP4. Organization of four groups was graphically described in Fig. 1.

Considering the whole database, the RU threshold scale was obtained by adding and subtracting half the standard deviation to average sample of rumination sub-scale among the participants' scales of CERQ, and then, high/low RU tendency was decided into GP1 and GP2. Similarly, high/low CD tendency was determined by adding and subtracting half the standard deviation to the average sample of positive refocusing sub-scales in these groups. The identical procedure was also followed in deciding high/low tendency of SE and CR in GP3 and GP4. Each group included 15 adults.

EEG Data Collection and Pre-Processing

Resting-state EEG series were recorded from scalp surface of the awake participants seated in front of a computer screen. 61-channel surface EEG recordings and VEOG recordings (61 scalp electrodes plus 1 electrode recording the VEOG below the right eye) are provided into 16 blocks of 60 sec in eyes-opened (8 blocks) and eyes-closed (8 blocks) states that interleaved to each other in data repository (Babayan et al., 2019). These recording blocks are organized with presentation software (Neurobehavioral Systems Inc., Ver16.5, Berkeley, USA).

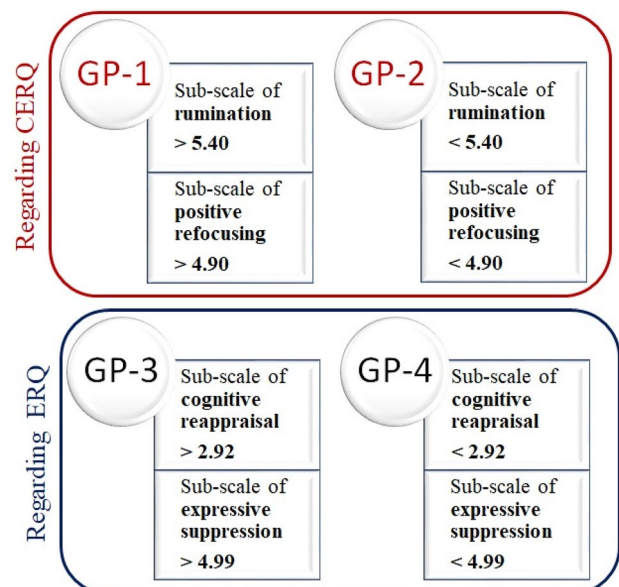


Fig. 1 Group organization with respect to individual's scores into questions in CERQ and ERQ

The artifacts originated from eye blink have spikes shape with the frequency lower than 4 Hz. While, the artifacts originated from the eye movements have square shape with high propagation (Crespel et al., 2005). In the clinical interpretation these artifacts should be removed from EEG data. These physiological artifacts are removed from raw data, i.e. contaminated surface EEG measurements as described in reference (Vigon et al., 2000).

The participants looked at computer screen to arrange eyes-opened state (black cross presented on a white background). The recording equipment of Brain Products ActiCaps (GmbH, Gilching, Germany) is used to measure surface EEG series with international 10–20 extended electrode placement system. The reference electrode is linked to FCz and VEOG is placed below the right eye, while the ground is located at the sternum. The amplitude resolution is 0.1 μ Volt, electrode impedance is kept below 5 k Ω . The sampling frequency is 2500 Hz, however, the raw EEG data is down-sampled to 250 Hz. Eyes-opened surface EEG recordings were analyzed in the present study. Un-processed raw data was firstly extracted from the database.

Schematic representation of EEG analysis procedure is shown in Fig. 2. Considering each electrode pair, short

EEG segments of 2 sec were filtered by using an Infinite-Impulse-Response (IIR) filter with order of 35 in order to remove network noise at 60 Hz (Notch filtering). Later, three separate Finite Impulse Response (FIR) filters were used to obtain full-band, Alpha-band and Beta-band frequency intervals of short segments. Applied IIR filter specifications are given in Table 5 in Appendix. More detailed optimization on IIR filter parameters can also be obtained by using optimization algorithms as described in reference (Mohammadi et al., 2021).

The frequency intervals were arranged as follows: In extracting full-band EEG segment, 1st stop-band and pass-band frequencies are 0.5 Hz and 1 Hz, 2nd pass-band and stop-band frequencies are 40 Hz and 40.5 Hz. In extracting Alpha-band interval of an EEG segment, 1st stop-band and pass-band frequencies are 7.5 Hz and 8 Hz, 2nd pass-band and stop-band frequencies are 11.5 Hz and 12 Hz. In extraction Beta-band interval of an EEG segment, 1st stop-band and pass-band frequencies are 12.5 Hz and 13 Hz, 2nd pass-band and stop-band frequencies are 29.5 Hz and 30 Hz. The obtained results confirm the use of mean alpha level as a measure of resting-state arousal under eyes-closed and eyes-open conditions (Barry et al., 2007).

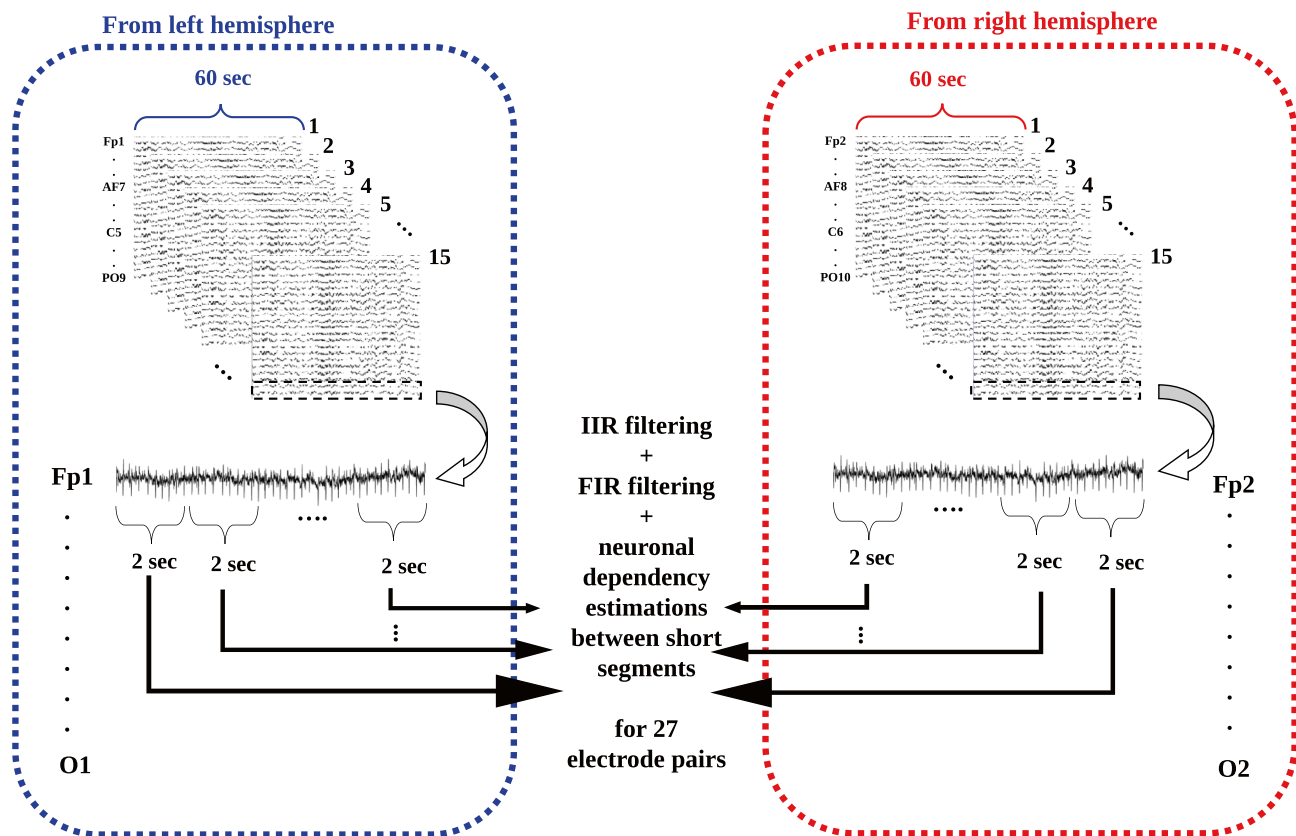


Fig. 2 Schematic representation of EEG analysis in computing inter-hemispheric neuro-functional dependency estimations

Inter-Hemispheric Neuronal Dependency Estimators

Scalp EEG series capture postsynaptic voltage variations in the cortex through surface electrodes in accordance with the standardized guideline of international 10–20 electrode-placement system. In the present study, neuro-electrical dependency between symmetric cortical regions (frontal, central, temporal, parietal and occipital) has been quantified in order to understand the brain network mechanism emerged from individual cognitive skills in terms of cognitive emotion regulation strategy. For this purpose, inter-hemispheric neuronal dependency between electrode pairs placed on scalp symmetrically in a specified cortical region as shown in Fig. 3.

Four dependency approach are examined to estimate inter-hemispheric EEG connectivity between right and left cortical neural populations in full-band (0.5 – 40.5 Hz), Alpha-band (7.5 – 12 Hz) and Beta-band (12.5 – 30 Hz) frequency components.

In quantifying the functional relationships between two EEG segments recorded from right and left cortical sites, COH function is based on cross-spectral analysis. COH gives magnitude-squared coherence as the normalization of the cross-power spectrum as follow,

$$COH_{xy} = \frac{|P_{xy}|}{\sqrt{P_{xx} \cdot P_{yy}}} \tag{1}$$

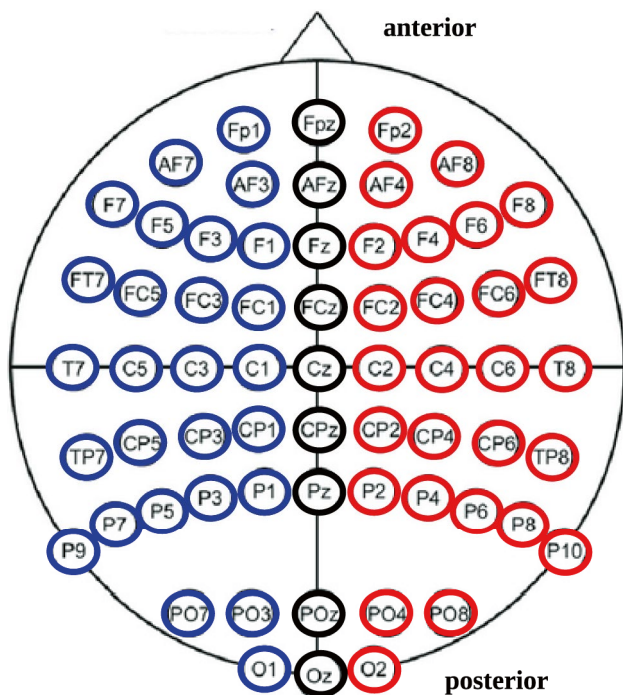


Fig. 3 The right (in red) and left (in blue) electrode placements over 62-channel EEG recording system

Here, the magnitude squared of the power spectral density estimations in accordance with band specific intervals of two EEG segments, x and y , are given by P_{xx} and P_{yy} . In addition, P_{xy} refers cross-power spectral density estimation between x and y . The increased functional connectivity is indicated by the high COH value. In other words, high EEG coherence implies dependent activation characterized by well-synchrony between symmetric neuronal populations at the cerebral cortex while low coherence indicates independence. COH is a frequency-dependent measure of the degree of linear relatedness between two-symmetric cortical locations. In detail, the resulting COH values indicate the magnitude of correlation between the respective amplitudes derived for a given frequency interval of two EEG segments.

In contrast to coherence, PLV is nonlinear inter-hemispheric dependency approach (Aviyente et al., 2011). The phase time courses of two time series, x and y (i.e. short segments of EEG series recorded from right and left cortical regions) are referred by ϕ_x and ϕ_y in estimating PLV as follow,

$$PLV_{xy}^i = \frac{1}{N} \exp j(\phi_x - \phi_y) \tag{2}$$

Thus, the corresponding phase difference is $\Delta\phi = \phi_x - \phi_y$. In case of well-synchrony between x and y (rise and fall together or with a certain lag), PLV is equal to 1, since $\Delta\phi$ will be consistent. In case of no relationship between x and y , PLV is equal to zero, since $\Delta\phi$ will be random. Therefore, PLV can be considered as a measure of segment-to-segment variability in terms of relative phase difference between x and y .

Comparing COH and PLV, COH may also be interpreted as a measure for stability of phase difference between identical frequency components of two simultaneously recorded EEG segments. Therefore, the higher COH values mean high cooperation and/or synchronization between underlying EEG recording sites.

Additionally, further knowledge on the dynamic behavior of synchronization processes assessed by the measurement of direction (time delay) and speed of information transfer between brain areas is significant. Information on these parameters can be obtained by the calculation of phase relations between oscillatory components of two signals. Phase and coherence are, mathematically, closely connected spectral parameters, and interpretation of phase is only sensible with sufficiently high coherence values. The cross-phase spectrum provides information on the time relationships between two EEG signals as a function of frequency.

Information Theory introduces MI to quantify the statistical correlation between two time series based on information transfer. Its algorithm can estimate how much information one of these two series will have about how the other series will change depending on this information. MI estimates the

information gained about x by measuring the y with probability distribution of amplitudes given by P_{x_i} and P_{y_j} , respectively (David et al., 2004). Then, it is possible to obtain the probability that the instantaneous values of x and y from two sources, related to each other, occur relative to the other as follow,

$$MI_{x,y} = H(X) + H(Y) - H(X, Y) \tag{3}$$

where $H(\cdot)$ denotes average amount of information derived from Shannon information theory in form,

$$H(X) = \sum_{x_i} P_{x_i} \log (P_{x_i}) \tag{4}$$

If there is no relative relation between x and y , the resulting value of MI is equal to zero, while MI is equal to 1 in case of high relative behavior between x and y .

WC is defined as cross-coherence between two short EEG segments (x and y) in units of normalized variance (Chang & Glover, 2010). Wavelet Transform (WT) is applied to time series in computing WC as follow,

$$WC_{x,y}(\tau, s) = WT_x(\tau, s)WT_y(\tau, s)^* \tag{5}$$

Here, WT_x and WT_y refer WT representations of x and y , respectively. Scaled versions of a mother wavelet denoted by $\Psi(t) = \pi^{-1/4} e^{j\omega t} e^{-0.5t^2}$ is convolved by time series (x or y) in obtaining WT in form,

$$WT_x(\tau, s) = \frac{1}{\sqrt{s}} \int_{-\infty}^{+\infty} x(t)\Psi^* \frac{t-\tau}{s} ds \tag{6}$$

Here, the parameters of τ and s denote the scale and translation. The wavelet function, $\Psi \in L^2(R)$ implies a zero average $\int_{-\infty}^{+\infty} \Psi(t)dt = 0$ and $*$ refers complex conjugation. Different frequency components of x is extracted via adjusting the scale, while translation (τ) correspond to time variations (Sankari et al., 2012).

Classification of Groups: Adaptive Boosting

Adaptive Boosting (Adaboost), is an ensemble method in supervised machine learning. The weights are re-assigned to each instance with higher weights to incorrectly

classified instances in Adaboost. The bias and variance are both reduced through boosting principle with high performance of decision trees on binary classification problems. Except for the first learner, each subsequent learner is converted as strong learners. For implementation of Adaptive Boosting, Statistics and Machine Learning Toolbox was used in MATLAB-2020a. 5-fold cross-validation was implemented with learning rate of 0.01. The number of learning cycles was empirically chosen as 30. In generating decision tree, 4 surrogate splits is used to improve the tree accuracy. In particular merge-leave is also used in generating decision tree (the decision tree merges leaves that originate from the same parent node, giving the sum of risk values equal to or greater than the risk associated with the parent node).

Due to low relatively low number of features in groups, deep learning models have not been used in the present study, although their popular use in both emotion recognition (Aydın, 2020; Chen & Hao, 2021; Oliveira & Praça, 2021) and object recognition in image processing (Yan et al., 2020a; Yan et al., 2020b; Yan et al., 2021).

Results

In each group, four approaches (COH, PLV, MI, WCOH) were examined for estimation of inter-hemispheric dependency features from 60 non-overlapped EEG segments of 2 sec over a trial of 2 min (Fig. 2) for 27 electrode pairs (Fig. 3) for 15 individuals. Then, the feature dimension was commonly 27 in both instant classification and subject-classification steps with respect to specified frequency interval. However, individuals were identified by ensemble averaging of dependency estimations from short segments in subject-classification for each frequency specification.

Regarding classification of GP1 and GP2 in accordance with dependency estimators in frequency specifications, 5-fold cross-validated adaboost classification provided performance variations as listed Table 1 in terms of Classification Accuracy (CA) in percent. Instant classification provided the higher performance in comparison to subject-classification in each frequency specification for each dependency estimator. The best results were obtained by

Table 1 Classification Accuracy (%) in classifying GP1 and GP2 with respect to inter-hemispheric connectivity estimations

	GP1 vs GP2					
	instant classification			subject classification		
	full-band	Alpha	Beta	full-band	Alpha	Beta
COH	99.44	66.67	90.00	63.33	64.44	68.88
PLV	97.22	90.00	83.33	80.00	63.33	83.33
MI	80.00	90.00	86.67	74.44	89.44	87.22
WCOH	74.11	69.33	64.22	60.00	53.33	53.33

Table 2 Classification Accuracy (%) in classifying G3 and G4 with respect to inter-hemispheric connectivity estimations

	GP3 vs GP4					
	instant classification			subject classification		
	full-band	Alpha	Beta	full-band	Alpha	Beta
COH	98.33	80.00	96.67	56.67	62.22	62.22
PLV	95.55	84.44	88.88	66.67	80.00	73.33
MI	96.67	96.67	93.33	71.11	83.33	84.44
WCOH	68.39	75.28	72.94	53.33	56.67	56.67

using COH and PLV, however the highest CA of 99.44% was provided by full-band specific COH estimations in instant classification.

Table 2 includes the classification performance list resulting from 5-fold cross-validated adaboost classifications of GP3 and GP4 in accordance with dependency estimators in frequency specifications. Relatively better results were obtained through instant classification in comparison to subject-classification. Both COH and PLV provided high performance in full-band intervals, while MI provided considerable high performance in each frequency specification. Besides, the highest CA of 98.33% was obtained by full-band specific COH estimations in instant classification. Comparing Tables 1 and 2, relatively better classification performances were observed in classifying G3 and G4 for each frequency specification.

Since the best results were obtained for non-averaged full-band specific COH estimations, the statistical error-bars of COH estimations in groups were shown in Figs. 4 and 5 in order to observe the difference between contrasting groups by visual inspection. The electrode pairs refer the cortical regions as given in Fig. 3. Graphical representations of full-band COH estimations showed that both GP1 and GP2 provided the higher values with the larger variations. In particular, GP3 provided the relatively lower values in comparison to GP4.

Considering full-band specific non-averaged COH estimations, one-way Anova test was used to quantify the statistically meaningful and significant differences between groups in terms of p-values ($p < 0.05$). As well, both spearman correlation coefficients (scc) and pearson correlation coefficients (pcc) was also computed for each electrode pair.

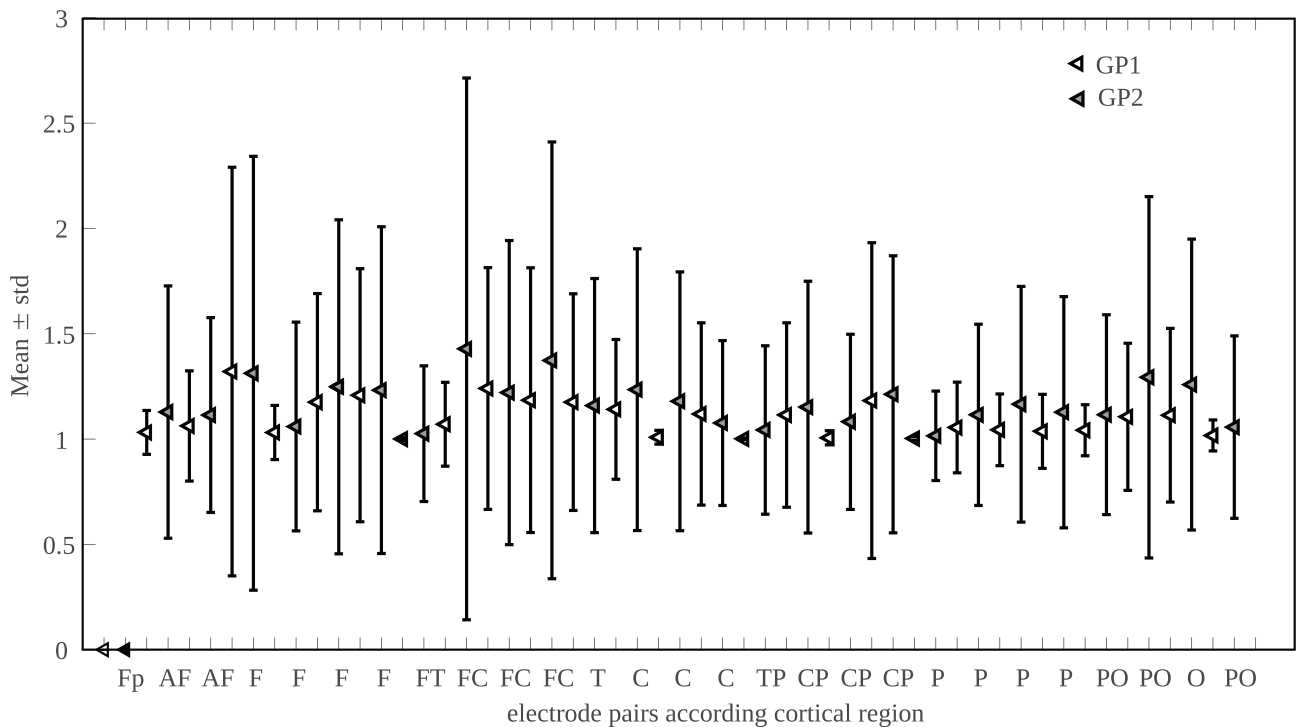


Fig. 4 Statistical error-bars in full-band COH estimations in GP1 and GP2: Electrode pairs are marked by cortical regions as Frontal (F), Central (C), Parietal (P), Occipital (O) and temporal (T)

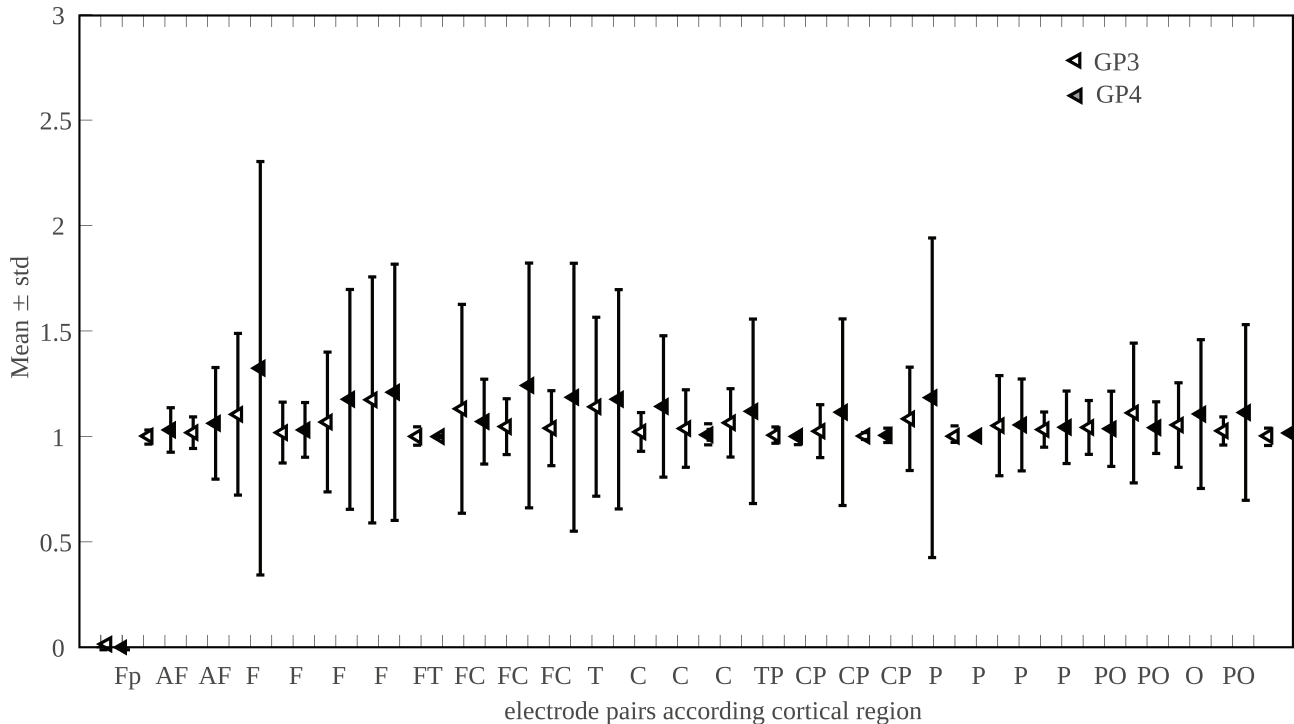


Fig. 5 Statistical error-bars in full-band COH estimations in GP3 and GP4: Electrode pairs are marked by cortical regions as Frontal (F), Central (C), Parietal (P), Occipital (O) and temporal (T)

The resulting statistical parameters were given in Table 3. A value of 0 implies that there is no linear correlation between the variables.

The value of p.c. can range from -1 to $+1$. Its negative value refers anti-linear-correlation between the groups at specified cortical regions. In detail, the stronger is either tendency, the larger is the absolute value of pcc. Thus, Table 3 showed that there was no strong correlation between the groups at most EEG recording sites. In particular, in both comparisons (GP1 vs GP2, GP3 vs GP4), negative p.c. values referred weak and anti-correlation between the groups. These results may indicate that full-band COH estimations of the contrasting groups may tend to be in the opposite direction relative to each other (the group provides relatively high COH estimations where the opposite group provides the relatively lower COH estimations). These quantitative results as listed in Table 3 were compatible with visual representation of statistical full-band COH estimations in groups as shown in Figs. 4 and 5.

Statistical one-way Anova test results in addition to pearson correlation and spearman correlation estimations were listed in Table 3 in comparing the groups: Mostly frontal, central and parietal regions provide meaningful and significant differences between GP1 and GP2. Regarding GP3 vs GP4, the lower number of regions provided statistically significant group differences at frontal, central and parieto-occipital regions. In detail, particular Brodmann areas of

1, 2, 5, 6, 7, 8, 9, 10, 18, 19, 20, 37, 39, 40, 41, 42, 46, 47 showed full-band coherence changes dependent on using rumination and distraction (GP1 vs GP2). The particular Brodmann areas of 2, 5, 6, 8, 9, 18, 20, 21, 37, 39, 40, 41, 42, 44, 47 and Broca showed full-band EEG coherence variations dependent on using suppression and reappraisal (GP3 vs GP4). Those differences were shown in Fig. 6 where the particular BAs that provided statistical differences between two-groups were coloured.

Discussion

In the present study, eyes-opened resting state surface EEG measurements were analyzed in order to investigate the possible cross-relation between inter-hemispheric neuronal coherence levels and contrasting cognitive emotion management skills. For this purpose, the features were computed by applying four different functional connectivity metrics to full-band, Alpha-band and Beta-band intervals of EEG series.

Regarding the use of spectral COH in comparison to PLV in discrimination of diversity between individuals having diverse cognitive skills or mental well-being, the application parameters as well as data collection procedures differ from each other as listed in Table 4. The highest number of EEG recording channels are considered in the present study

Table 3 Statistical test results in p-value, scc and pcc in comparing the groups in accordance with full-band COH estimations with respect to both electrode pairs (e.p.) and Brodmann Areas (BAs)

BAs	e.p.	GP1 vs GP2			GP3 vs GP4		
		p-value	scc	pcc	p-value	scc	pcc
10/10	(1) Fp1-2	0.6e-10	0.191	-0.027	0.7540	0.010	-0.021
09/09	(2) AF3-4	0.1e-5	0.210	-0.043	0.0470	0.321	-0.013
46/46	(3) AF7-8	0.0035	0.275	-0.009	0.0004	0.302	-0.009
47/45	(4) F7-8	0.8521	-0.327	-0.067	0.0038	-0.056	-0.065
46/46	(5) F5-6	0.0987	-0.285	-0.026	0.0705	0.022	0.003
08/08	(6) F3-4	0.0201	0.232	0.253	0.3204	-0.140	-0.001
08/08	(7) F1-2	0.4604	0.126	-0.020	0.0354	-0.080	0.078
06/06	(8) FC1-2	0.0164	-0.072	-0.002	0.0121	-0.180	-0.026
06/06	(9) FC3-4	0.1e-10	0.047	-0.085	0.6869	-0.089	-0.067
Broca/44	(10) FC5-6	0.5252	-0.360	-0.106	0.1e-4	0.328	0.052
47/47	(11) FT7-8	0.3e-5	0.319	-0.073	0.0002	-0.144	-0.037
42/21	(12) T7-8	0.5400	0.133	-0.056	0.4449	-0.138	-0.053
42/41	(13) C5-6	0.0001	0.171	0.029	0.1e-6	0.135	-0.046
02/01	(14) C3-4	0.1e-10	0.382	-0.040	0.2010	-0.105	-0.024
05/05	(15) C1-2	0.0291	0.152	-0.031	0.2883	0.161	0.051
05/05	(16) CP1-2	0.0016	-0.123	-0.033	0.0293	-0.075	-0.016
02/40	(17) CP3-4	0.1304	0.117	-0.029	0.0042	0.091	-0.030
40/40	(18) CP5-6	0.5e-7	0.274	-0.015	0.0453	-0.073	-0.011
21/21	(19) TP7-8	0.3683	0.154	-0.054	0.0192	0.106	-0.003
37/37	(20) P7-8	0.0789	-0.136	-0.022	0.0751	0.126	-0.004
39/39	(21) P5-6	0.0001	0.084	-0.024	0.2560	0.195	-0.013
39/39	(22) P3-4	0.5e-9	0.149	-0.041	0.0026	-0.499	-0.066
07/07	(23) P1-2	0.2e-5	0.007	0.004	0.2010	-0.111	-0.043
19/19	(24) PO3-4	0.6e-5	0.115	-0.044	0.1561	-0.052	-0.053
19/19	(25) PO7-8	0.1e-8	-0.094	-0.074	0.0731	-0.089	0.009
20/37	(26) P9-10	0.6e-7	-0.090	-0.057	0.7e-4	-0.074	-0.024
18/18	(27) O1-2	0.0068	-0.037	-0.024	0.0081	-0.009	0.215

for classification of contrasting cognitive abilities in healthy individuals. Raw data is primarily filtered by an IIR-Notch filter and short non-overlapped EEG segments are filtered by

three FIR filters in extracting full-band (0.5-40.5 Hz), alpha-band and beta-band in EO state, while BP is the mostly used pre-filter in other studies in Table 4. The largest recording

Fig. 6 Particular BAs provided clear statistical differences between contrasting groups in accordance with full-band COH estimations

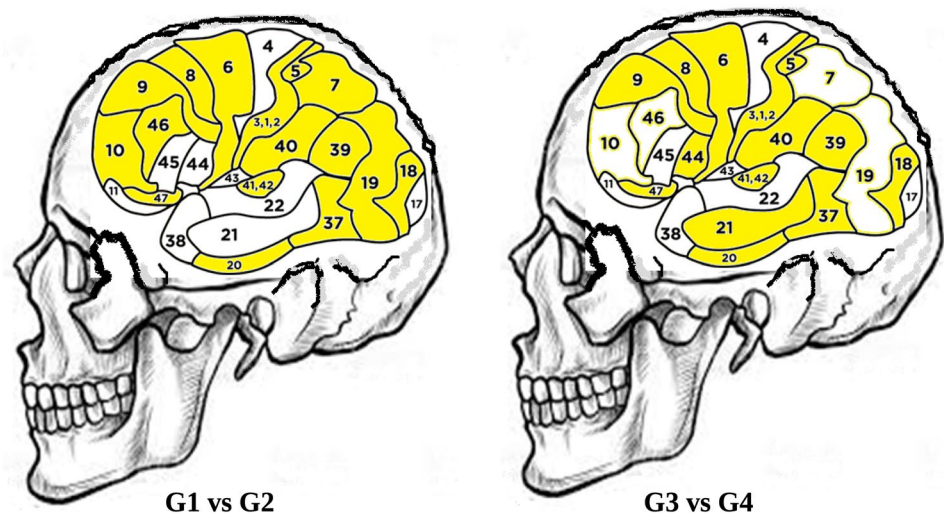


Table 4 Brief review on the studies that analyze resting-state or sleep EEG without any stimulus by examining both spectral COH and PLV in discriminating cognitive or mental diversity in subjects with respect to sampling frequency (s.f.) in Hz, number of recording channels (n.c.), analyzed frequency interval (f.i.), pre-filtering of raw data,

ref.	content	n.c.	s.f.	pre-filtering	state	length	method	indicator
current	cognitive	62	250	IIR, FIR	EO	2min, 2sec	BM	na., no.e
Handayani et al. (2018)	cognitive	14	128	BP	EC	20min, 8sec	WM, PM	ga., 50% o.e.
Bob and Palus (2008)	cognitive	32	1000	BP	EC	5min, 16sec	WT	ga, no.e
Dell'Acqua et al. (2021)	mental	32	500	BP	EO	4min, 4sec	WM, PM	ga, 75% o.e.
Zhang et al. (2014)	mental	32	250	BP	EC	1min, 10sec	WM, PM,	ga, 50% o.e.
Gomez et al. (2021)	coma	19	256	BP	coma	120h, 5min	FT	na., no.e
Hussain et al. (2018)	eyes-state	19	200	LP	EC, EO	2.5min	WT	absolute wavelet power
Mezeiova and Palus (2012)	sleep-stage	6	256	HP, LP	sleep	5h, 30sec	FT	ga, no.e

subject state (eyes-opened, eyes-closed, sleep, coma), the length of analysis interval and segment, the method used in computing spectral coherence and quantitative indicator as non-averaged (na.) or grand-averaged (ga.) estimations from non-overlapped epochs (no.e) or overlapped epochs (o.e.)

interval (120h) and the largest EEG segments are examined in reference study to estimate the outcome of postanoxic coma (Gomez et al., 2021). In this study, the dependency metrics (COH, PLV, MI) are combined to determine a huge feature set, then, classifiers are trained with non-averaged estimations from segments of 5min over 120h. In both Handayani et al., 2018 and Zhang et al., 2014, the individuals are identified by the grand averaged estimations from 50% overlapped long segments (8sec and 10sec). As well, inter-hemispheric functional indicator is defined as the grand averaged dependency estimations from 75% overlapped shorter segments (4sec) in (Dell'Acqua et al., 2021). In the present study, cognitive abilities are identified by non-averaged dependency estimations from non-overlapped short segments (2sec) over 2min rather than the identification of individuals with averaged estimations from overlapped longer segments. In computing spectral COH values, most the studies commonly use WM in combination with PM (Handayani et al., 2018; Dell'Acqua et al., 2021; Zhang et al., 2014), while the others use either FT (Gomez et al., 2021; Mezeiova & Palus, 2012) or WT (Bob & Palus, 2008; Hussain et al., 2018). In the present study, BM is used to estimate spectral COH values based on the assumption that short EEG segments can be modeled by an Auto-Regressive model. So, the COH estimations provided the best results in classification of contrasting cognitive skills.

Table 5 IIR filtering specifications with variables

Variables	Meaning	Value
Q	the quality factor	35
den	density factor	20
wo	the notch frequency	60/Fs/2
BW	band width	wo/35
r	pass-band ripple	0.05750
ρ_1	1st stop-band attenuation	0.001
ρ_2	2nd stop-band attenuation	0.0001

In analysis of resting-state surface EEG measurements, the following specifications can be proposed:

- the length of EEG segment should be short as 2sec due to nerve action potential generation and propagation mechanism in addition to post-synaptic neurotransmitter transition during rest without any stimulus.
- FIR filter should be used to extract specific frequency interval with sensitive and realistic filtering parameters
- Short EEG segments can be assumed to be modeled by Auto-Regressive model
- Averaging process cause loss of information in long EEG measurements due to time-varying post-synaptic potential variations across the cortex. Therefore, non-averaged inter-hemispheric dependency estimations should be used as indicators in detecting specific cognitive or mental states.

Conclusion

The functional connectivity approaches are as follow: 1. coherence based on power spectral density estimation, 2. PLV based on phase difference between neuro-electrical activities generated by neuronal populations at right and left hemispheres, 3. MI based on statistical alterations throughout time instants in those neuro-electrical activities, and 4. WCOH based on wavelet transformed coefficients of those neuro-electrical activities.

Two groups include the individuals who use frequently and rarely use of both rumination and distraction (GP1 and GP2), the other groups include the individuals who use frequently and rarely use of both expressive suppression and reappraisal (GP3 and GP4). Thus, the groups (GP1 vs GP2, GP3 vs GP4) were classified by examining Adaboost classifiers with respect to non-averaged inter-hemispheric

connectivity estimations from short-segments of 2 *sec* as well as ensemble averaged of the estimations over a trial of 2 *min* for 27 electrode pairs excluding middle-line sites and reference points as shown in Fig. 3. The resulting Classification Accuracies reveal that full-band coherence estimations provide the most meaningful and discriminative indicators in quantifying inter-hemispheric neuro-electrical synchronicity in resting state. Besides, ensemble averaging connectivity estimations over a trial of 2 *min* did not provide clear difference between contrasting groups. Due to nature of ongoing EEG series originated from spontaneous and time-varying brain functions, it is superior to determine a collection of coherence estimations as the large number of features in association with consecutive small-windows of 2 *sec* in a recording interval of 2 *min*.

GP1 and GP2 were successfully classified with high CA of 99.44%, GP3 and GP4 were successfully classified with high CA of 98.33% by using Adaboost classifiers driven by non-averaged full-band (0.5 – 40.5 *Hz*) EEG coherence estimations. Regarding the statistical test results and corresponding EEG recording sites, more cortical regions are affected by ruminative thoughts by means of inter-hemispheric EEG coherence in comparison to optimistic thoughts. However, the findings reveal that particular BAs of 2, 5, 6, 8, 9, 18, 20, 37, 39, 40, 41, 42, 47 were commonly found to be sensitive to cognitive emotion management strategies in healthy adults. The main functions of these BAs are as follow:

- 2 sensory perception, motor learning (primary somatosensory cortex)
- 5 working memory, language processing, visuo-motor attention, pain perception, tactile localization, motor execution, bimanual manipulation, (somatosensory association cortex)
- 6 memory-language-motor functions, planning and sensory guidance of both muscle movement and complex motor movements (premotor cortex and supplementary motor cortex)
- 8 spatial memory, memory-guided saccades (prefrontal cortex)
- 9 working memory, planning, organization, and regulation of motor functions, sustaining attention (dorso-lateral prefrontal cortex)
- 18 visual depth perception through receiving input from primary visual cortex, (secondary visual cortex).
- 20 visual fixation, identify intention (Inferior temporal gyrus)
- 37 processing of color information, recognition of face/body/word/numbers through visual perception, (occipito-temporal cortex)
- 39 speech fluency, language comprehension, (Angular gyrus, part of Wernicke’s area)
- 40 speech fluency, language comprehension, (Supramarginal gyrus, part of Wernicke’s area)
- 41/2 auditory working memory, Visual speech perception, (primary and secondary auditory cortex)
- 47 working and episodic memory, management of reward and conflict, spoken language, language semantics, identifying semantics, processing of linguistic information, (orbital part of inferior frontal gyrus).

In conclusion, overall results reveal that CERs are highly correlated with main associative brain functions such as working memory, visual/sensory perception and cognition. As well, expressive suppression cause decrease in full-band EEG coherence at mostly fronto-central regions. The reason of this findings may originated from lack of experience of positive emotions, since frequently use of SE increases the felt intensity of negative emotions, while reduces the felt of positive emotions, such as happiness as discussed in reference (Gross & Jazaieri, 2014).

Information Sharing Statement

Raw data is openly available and is distributed along with the a data repository so called LEMON described in reference (Babayan et al., 2019).

Abbreviations EEG: Electro-Encephalo-Gram; CERs: Cognitive Emotion Regulation strategies; ERQ: Emotion Regulation Questionnaire; CERQ: Cognitive Emotion Regulation Questionnaire; RU: Rumination (an emotion regulation strategy identified through CERQ); CD: Cognitive Distraction (an emotion regulation strategy identified through CERQ); ER: Expressive Suppression (an emotion regulation strategy identified through ERQ); CR: Cognitive Reappraisal (an emotion regulation strategy identified through ERQ); IIR: Infinite Impulse Response; FIR: Finite Impulse Response; FCz: Reference electrode placed on the midline sagittal plane of the skull as Fronto-Central-zero; VEOG: Vertical Electro-Oculo-Gram in recording electrical activity, i.e. artifacts produced by eye blinks or eye movement; COH: Spectral Coherence based on spectral density estimation by using Burg Method; WCOH: Wavelet Transform based COherence based on Wavelet Transform; PLV: Phase Locking Value; MI: Mutual Information; Fs: Sampling Frequency; CA: Classification Accuracy; WM: Welch’s Method; PM: Periodogram Method; WT: Wavelet Transform; FT: Fourier Transform; Hz: Hertz in frequency; sec: second in time; min: minutes in time; BAs: Brodman Areas; E.O: eyes-opened; r.s.: resting-state; s.l.: segment length; n.c.: number of EEG recording channels; e.p.: electrode placement; scc: statistical spearman correlation coefficient; pcc: statistical pearson correlation coefficient; BP: band-pass filtering; LP: low-pass filtering; HP: high-pass filtering

Data Availability EEG data was downloaded from a publicly available data-set at following web page: http://fcon_1000.projects.nitrc.org/indi/retro/MPI_LEMON/downloads/download_EEG.html. As well, the participants’ scores in both ERQ and CERQ are available at the following web-page under the title of ‘Behavioural Data’ https://www.fcon_1000.projects.nitrc.org/indi/retro/MPI_LEMON.html.

Declarations

Conflict of Interest The author declares that she has no conflict of interest.

References

- Abler, B., & Kessler, H. (2009). Emotion Regulation Questionnaire - Eine deutsche Version des ERQ von Gross and John. *Diagnostica*, 55(3), 144–152. <https://doi.org/10.1026/0012-1924.55.3.144>.
- Aviyente, S., Bernat, E. M., et al. (2011). A phase synchrony measure for quantifying dynamic functional integration in the brain. *Human Brain Mapping*, 32(01), 80–93.
- Aydin, S. (2020). Deep learning classification of neuro-emotional phase domain complexity levels induced by affective video film clips. *IEEE Journal of Biomedical and Health Informatics*, 24(6), 1695–1702. <https://doi.org/10.1109/JBHI.2019.2959843>.
- Aydin, S., Tunga, M. A., & Yetkin, S. (2015). Mutual Information analysis of sleep EEG in detecting psycho-physiological insomnia. *Journal of Medical Systems*. <https://doi.org/10.1007/s10916-015-0219-1>.
- Aydore, S., Pantazis, D., Leahy, R. M. (2013). A note on the phase locking value and its properties. *NeuroImage*, 74, 231–244. <https://doi.org/10.1016/j.neuroimage.2013.02.008>.
- Babayan, A., Erbey, M., Kumral, D., et al. (2019). Data Descriptor: A mind-brainbody dataset of MRI EEG, cognition, emotion, and peripheral physiology in young and old adults. *Scientific Data*, 6(1), 180308.
- Barry, R., et al. (2007). EEG differences between eyes-closed and eyes-open resting conditions. *Clinical Neurophysiology*, 118(12), 2765–73. <https://doi.org/10.1016/j.clinph.2007.07.028>.
- Bob, P., & Palus, M. (2008). EEG phase synchronization in patients with paranoid schizophrenia. *Neuroscience Letters*, 447(1), 73–7. <https://doi.org/10.1016/j.neulet.2008.09.055>.
- Bosman, C. A., Schoffelen, J.-M., Brunet, N., Oostenveld, R., Bastos, A. M., Womelsdorf, T., et al. (2012). Attentional stimulus selection through selective synchronization between monkey visual areas. *Neuron*, 75, 875–888. <https://doi.org/10.1016/j.neuron.2012.06.037>.
- Buhle, J. T., Silvers, J. A., Wager, T. D., et al. (2014). Cognitive reappraisal of emotion: a meta-analysis of human neuroimaging studies. *Cerebral Cortex*, 24, 2981–2990. <https://doi.org/10.1093/cercor/bht154>.
- Chang, C., & Glover, G. H. (2010). Time-frequency dynamics of resting-state brain connectivity measured with fMRI. *Neuroimage*, 50(1), 81–98. <https://doi.org/10.1016/j.neuroimage.2009.12.011>.
- Chen, M., & Hao, Y. (2021). Label-less Learning for Emotion Cognition. *IEEE Transactions on Neural Networks and Learning System*, 31(7), 2430–2440. <https://doi.org/10.1109/TNNLS.2019.2929071>.
- Crespel, A., Gélisse, P., et al. (2005) Atlas of Electroencephalography, vol.1, J. Libbey Eurotext, Paris, France, 1st ed.
- David, O., Cosmelli, D., & Friston, K. J. (2004). Evaluation of different measures of functional connectivity using a neural mass model. *Neuroimage*, 21(02), 659–673. <https://doi.org/10.1016/j.neuroimage.2003.10.006>.
- Dell’Acqua, C., et al. (2021). Increased functional connectivity within alpha and theta frequency bands in dysphoria A resting-state EEG study. *Journal of Affective Disorders*. <https://doi.org/10.1016/j.jad.2020.12.015>.
- Diekhof, E. K., Geier, K., et al. (2011). Fear is only as deep as the mind allows. *Neuroimage*, 58, 275–285. <https://doi.org/10.1016/j.neuroimage.2011.05.073>.
- Garnefski, N., Kraaij, V., Spinhoven, P. (2001). Negative life events, cognitive emotion regulation and emotional problems. *Personality and Individual Differences*, 30(8), 1311–1327. [https://doi.org/10.1016/S0191-8869\(00\)00113-6](https://doi.org/10.1016/S0191-8869(00)00113-6).
- Giuliani, N. R., Drabant, E. M., et al. (2011). Emotion regulation and brain plasticity: expressive suppression use predicts anterior insula volume. *Neuroimage*, 58, 10–15. <https://doi.org/10.1016/j.neuroimage.2011.06.028>.
- Giuliani, N. R., Drabant, E. M., & Gross, J. J. (2011). Anterior cingulate cortex volume and emotion regulation: is bigger better? *Biological Psychology*, 86, 379–382. <https://doi.org/10.1016/j.biopsycho.2010.11.010>.
- Goldin, P. R., McRae, K., Ramel, W., & Gross, J. J. (2008). The neural bases of emotion regulation: reappraisal and suppression of negative emotion. *Biological Psychiatry*, 63, 577–586.
- Gomez, M. C., Kejyer, H. M., et al. (2021). EEG functional connectivity contributes to outcome prediction of postanoxic coma. *Clinical Neurophysiology*. <https://doi.org/10.1016/j.clinph.2021.02.011>.
- Gross, J. J. (2002). Emotion regulation: affective, cognitive, and social consequences. *Psychophysiology*, 39(3), 281–91.
- Gross, J. J., & Jazaieri, H. (2014). Emotion, emotion regulation, and psychopathology: An affective science perspective. *Clinical Psychological Science*, 2, 387–401. <https://doi.org/10.1177/2167702614536164>.
- Gross, J. J., & John, O. P. (2003). Individual differences in two emotion regulation processes: implications for affect, relationships, and well-being. *Journal of Personality and Social Psychology*, 85(2), 348. <https://doi.org/10.1037/0022-3514.85.2.348>.
- Handayani, et al. (2018). Coherence and phase synchrony analyses of EEG signals in Mild.
- Hussain, L., Aziz, W., Saeed, S., Idris, A., Awan, I. A., Shah, S. A., ... & Rathore, S. (2018). Spatial wavelet-based coherence and coupling in EEG signals with eye open and closed during resting state. *IEEE Access*, 6, 37003–37022. <https://doi.org/10.1109/ACCESS.2018.2844303>.
- Jeonga, J., Goreb, J. C., & Petersona, B. S. (2001). Mutual information analysis of the EEG in patients with Alzheimer’s disease. *Clinical Neurophysiology*, 112, 827–835.
- Kalokerinos, E. K., Greenaway, K. H., & Denson, T. F. (2014). Emotion reappraisal but not suppression down regulates the experience of positive and negative emotion. *Emotion*, 15, 271–275. <https://doi.org/10.1037/emo0000025>.
- Lachaux, J. P., Lutz, A., Rudrauf, D., et al. (2002). Estimating the time-course of coherence between single-trial brain signals: an introduction to wavelet coherence. *Neurophysiologie Clinique*, 32(3), 157–74. [https://doi.org/10.1016/s0987-7053\(02\)00301-5](https://doi.org/10.1016/s0987-7053(02)00301-5).
- Le Van, Quyen M., Foucher, J., Lachaux, J., Rodriguez, E., Lutz, A., Martinerie, J., et al. (2001). Comparison of Hilbert transform and wavelet methods for the analysis of neuronal synchrony. *Journal of Neuroscience Methods*, 111, 83–98. [https://doi.org/10.1016/S0165-0270\(01\)00372-7](https://doi.org/10.1016/S0165-0270(01)00372-7).
- Lee, T. W., Dolan, R. J., & Critchley, H. D. (2008). Controlling emotional expression: behavioral and neural correlates of nonimitative emotional responses. *Cerebral Cortex*, 18, 104–113. <https://doi.org/10.1093/cercor/bhm035>.
- Loch, N., Hiller, W., Witthoef, M. (2011). The Cognitive Emotion Regulation Questionnaire (CERQ). Psychometric evaluation of a German adaptation. *Zeitschrift für Klinische Psychologie und Psychotherapie*, 40(2), 94–106. <https://doi.org/10.1026/1616-3443/a000079>.
- Mezeiova, K., & Palus, M. (2012). Comparison of coherence and phase synchronization of the human sleep electroencephalogram. *Clinical Neurophysiology*. <https://doi.org/10.1016/j.clinph.2012.01.016>.
- Mohammadi, A., Zahiri, S. H., et al. (2021). Design and modeling of adaptive IIR filtering systems using a weighted sum - variable length particle swarm optimization. *Applied Soft Computing*, 109, 107529. <https://doi.org/10.1016/j.asoc.2021.107529>.
- Na, S. H., Jin, S. H., Kim, S. Y., & Ham, B. J. (2002). EEG in schizophrenic patients: mutual information analysis. *Clinical Neurophysiology*, 113(12), 1954–1960. [https://doi.org/10.1016/S1388-2457\(02\)00197-9](https://doi.org/10.1016/S1388-2457(02)00197-9).

- Ochsner, K. N., & Gross, J. J. (2008). Cognitive emotion regulation: insights from social cognitive and affective neuroscience. *Current Directions in Psychological Science*, 17, 153–158.
- Oliveira, J., & Praça, I. (2021). On the usage of pre-trained speech recognition deep layers to detect emotions. *IEEE Access*, 9, 9699–9705. <https://doi.org/10.1109/ACCESS.2021.3051083>.
- Phan, K. L., Fitzgerald, D. A., et al. (2005). Neural substrates for voluntary suppression of negative affect: a functional magnetic resonance imaging study. *Biological Psychiatry*, 57, 210–219.
- Ramanand, P., Bruce, M. C., & Bruce, E. N. (2001). Mutual information analysis of EEG signals indicates age-related changes in cortical interdependence during sleep in middle-aged versus elderly women. *Journal of Clinical Neurophysiology*, 27(4), 274–284. <https://doi.org/10.1097/WNP.0b013e3181eaa9f5>.
- Ray, S., & Maunsell, J. H. R. (2010). Differences in gamma frequencies across visual cortex restrict their possible use in computation. *Neuron*, 67, 885–896. <https://doi.org/10.1016/j.neuron.2010.08.004>.
- Roberts, M. J., Lowet, E., Brunet, N. M., Ter Wal, M., Tiesinga, P., Fries, P., et al. (2013). Robust gamma coherence between macaque V1 and V2 by dynamic frequency matching. *Neuron*, Elsevier Inc., 78, 523–36. <https://doi.org/10.1016/j.neuron.2013.03.003>.
- Saalman, Y. B., Pinsk, M. A., Wang, L., Li, X., Kastner, S. (2012). The pulvinar regulates information transmission between cortical areas based on attention demands. *Science*, 753–756, <https://doi.org/10.1126/science.1223082>.
- Sankari, Z., Adeli, H., & Adeli, A. (2012). Wavelet coherence model for diagnosis of Alzheimer disease. *Clinical EEG and Neuroscience*, 43(4), 268–78. <https://doi.org/10.1177/1550059412444970>.
- Vigon, L., Saatchi, M.R., et al. (2000). Quantitative evaluation of techniques for ocular artefact filtering of EEG waveforms, *IEE Proc. of Science, Measurement and Tech.*, 147(5):219–228, 2000.
- Wang, K., Huang, H., et al. (2017). MRI correlates of interaction between gender and expressive suppression among the Chinese population. *Neuroscience*, 347, 76–84. <https://doi.org/10.1016/j.neuroscience>.
- Webb, T. L., Miles, E., & Sheeran, P. (2012). Dealing with feeling: a meta-analysis of the effectiveness of strategies derived from the process model of emotion regulation. *Psychological Bulletin*, 138(4), 775–808.
- Yan, C., Gong, B., et al. (2020). Deep multi-view enhancement hashing for image retrieval. *IEEE Transactions on Pattern Analysis and Machine Intelligence*. <https://doi.org/10.1109/TPAMI.2020.2975798>.
- Yan, C., Li, Z., et al. (2021). Depth image denoising using nuclear norm and learning graph model. *ACM Trans on Multimedia Comp: Comm. & Apps*. <https://doi.org/10.1145/3404374>.
- Yan, C., Shao, B., et al. (2020). 3D Room layout estimation from a single RGB image. *IEEE Transactions on Multimedia*. <https://doi.org/10.1109/TMM.2020.2967645>.
- Zhang, C., Yu, X., et al. (2014). Phase synchronization and spectral coherence analysis of EEG activity during mental fatigue. *Clinical EEG and Neuroscience*, 45(4), 249–256. <https://doi.org/10.1177/1550059413503961>.
- Zhang, X., Noah, J. A., Dravida, S., & Hirsch, J. (2020). Optimization of wavelet coherence analysis as a measure of neural synchrony during hyperscanning using functional near-infrared spectroscopy. *Neurophotonics*, 7(1), 016004. <https://doi.org/10.1117/1.NPh.7.1.015010>.
- Zhang, X., Yu, J., Zhao, R., Xu, W., et al. (2015). Activation detection in functional near-infrared spectroscopy by wavelet coherence. *Journal of Biomedical Optics*, 20(1), 016004. <https://doi.org/10.1117/1.JBO.20.1.016004>.

Publisher's Note Springer Nature remains neutral with regard to jurisdictional claims in published maps and institutional affiliations.